ANU-P/1067

STRUCTURE OF HIGH-SPIN ISOMERS IN TRANS-LEAD NUCLEI

(Invited Talk at the XXV Zakopane School on Physics 5-12 May 1990)

G.D. DRACOULIS

Department of Nuclear Physics, Research School of Physical Sciences,
Australian National University, GPO Box 4, Canberra, ACT 2601, Australia.

Invited Talk at the XXV Zakopane School on Physics, 5-12 May 1990

STRUCTURE OF HIGH-SPIN ISOMERS IN TRANS-LEAD NUCLEI

G.D. Dracoulis

Department of Nuclear Physics, Research School of Physical Sciences, Australian National University, PO Box 4, Canberra, ACT 2601, Australia

ABSTRACT: The structure of core-excited high-spin isomers in the $N \leq 126$ isotopes of At, Rn and Fr is reviewed. New results for high-spin states in ^{211}Rn and ^{212}Rn, approaching the limit of the available angular momentum from the valence particles, are presented. The recurring experimental feature is decay by very enhanced E3 transitions. These, and other properties are explained in a natural way by inclusion of particle-octupole vibration coupling, in a semi-empirical shell model. The deformed independent particle model is not successful in explaining these features.

PREFACE

This talk draws on results from a program of high spin spectroscopy of nuclei in the trans-lead region, carried out at the ANU over the last decade. As well as collecting previously published results, as referred to in the text, some results presented are from work in progress and to some extent preliminary in nature. The interpretation and results are the outcome of a continuing, collaborative effort and I would particularly like to acknowledge the contributions of Aidan Byrne, Alan Poletti, Andrew Stuchbery and Paul Davidson.

1. INTRODUCTION

The fascination excited nuclei states with directly measurable lifetimes, $\tau \geq$ few ns, have for experimentalists, is manifold. They allow accurate measurements of transition strengths; make practicable time-differential techniques for static and magnetic moments; allow unambiguous placement of transitions in nuclear level schemes through temporal ordering; substantially improve sensitivity to weakly populated states since spectrum complexity can be reduced by separation into

different time regions; and give the prospect of bootstrapping to high spin by identifying transitions preceding high-spin isomers.

The lifetime of a nuclear state depends in general on the transition energy ΔE and the relationship between it and the states to which it decays. Schematically we would write

$$1/\tau \;\alpha\; (\Delta E)^{2\lambda+1}\, |\langle f|\, T_\lambda\, |i\rangle|^2 \qquad (1)$$

If ΔE is small and the multipolarity is large the lifetime can be relatively long. This could be by chance, or because the upper state represented an unusually efficient way for the nucleus to carry angular momentum, hence, its relatively low energy and high spin. Alternatively, a long lifetime could signal a profound change in nuclear structure resulting in a small overlap because of the large configuration change (i.e. the re-arrangement of many orbits), or a shape change. A long lifetime, however, does not *necessarily* imply a small transition strength. For example, the single particle (Weiskopff) lifetime for electric octupole transitions is

$$\tau_{s.p.}\,(E3) = 1.752 \times 10^6 .\; 16.83/(A^2.E\gamma^7)\,(ns) \quad (E_\gamma \text{ in MeV}) \qquad (2)$$

corresponding to a 656 ns lifetime for a 1 MeV γ-ray in ^{212}Rn.

Nevertheless, there has been considerable enthusiasm since the early 70s for associating high-spin isomers with deformed "band-heads' of oblate equilibrium shape. These would be favoured in energy if the nucleus were polarised due to the congregation of a number of particles in the equatorial plane – a consequence of the alignment of high spin orbitals in an otherwise spherical nucleus.

Such yrast traps have been the subject of many theoretical studies[1-5], particularly in the context of the deformed independent particle model (DIPM). Even very recent reviews[5-7] associate core-excited yrast isomers with such moderately deformed ($\beta \sim -0.1$) configurations. Whilst this might be the appropriate description in the Gd region[8,9] it does not seem possible for the DIPM, without incorporation of an explicit octupole degree of freedom, to explain the distinguishing feature of many

such isomers in the trans-lead region – their decay by very enhanced (≥ 30 s.p.u.) E3 transitions.

2. CORE-EXCITED ISOMERS

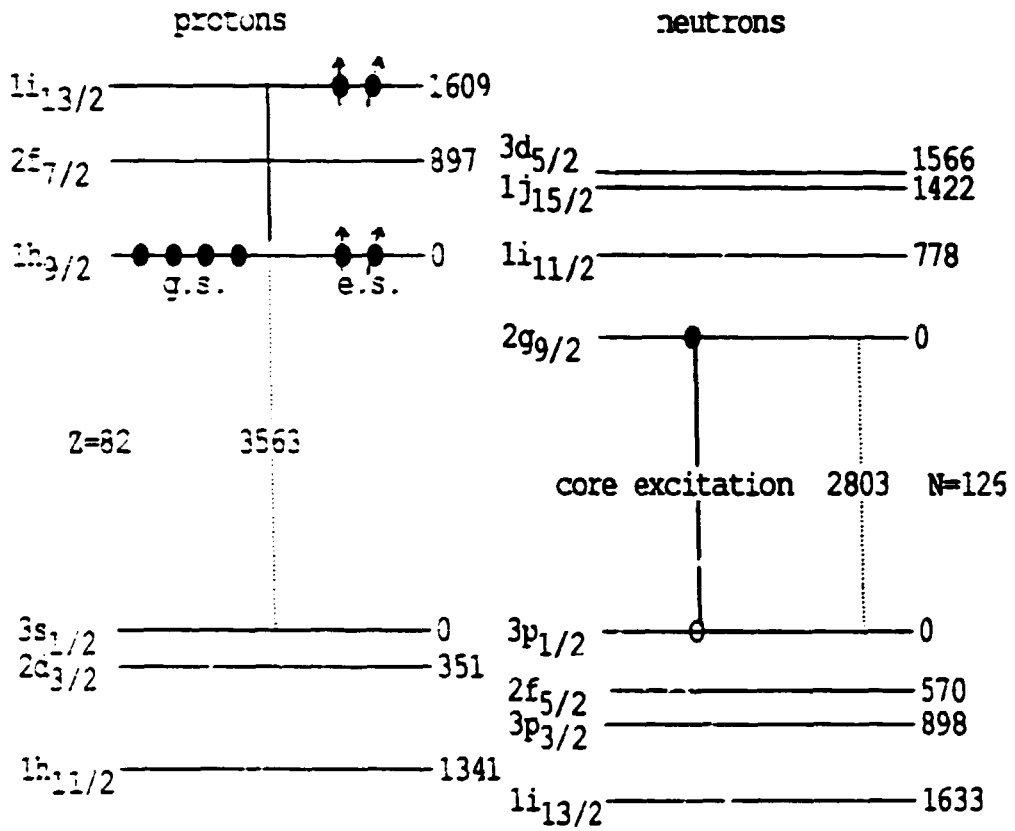

Figure 1

The yrast states below spin ~20ħ in the $_{86}$Rn nuclei with N ≤ 126 are formed by alignment of the four valence protons in the $h_{9/2}$, $f_{7/2}$ and $i_{13/2}$ orbitals. The last two form a "Δℓ = 3 pair" implying a large E3 coupling matrix element. An yrast 20^+ state from the $\pi\,[h^2_{9/2}\, i^2_{13/2}]_{20^+}$ configuration is commonly observed although a higher spin state, higher in energy, with the configuration $\pi[h_{9/2}\, i^3_{13/2}]_{21^-}$ could also be formed. To make even higher spins it is necessary to promote neutrons across the N = 126 shell gap from the low-spin orbitals ($p_{1/2}$, $p_{3/2}$ and $f_{5/2}$) into the $g_{9/2}$, $i_{11/2}$ and $j_{15/2}$ "valence" orbitals, as shown in figure 1. The $g_{9/2}$ and $j_{15/2}$ orbitals also form a Δℓ=3 pair.

2.1 Residual Interactions

Although the core-excitation costs about 2.8 MeV a considerable proportion can be retrieved through the strongly attractive interaction acting between mutually aligned, high-spin protons and neutrons (in

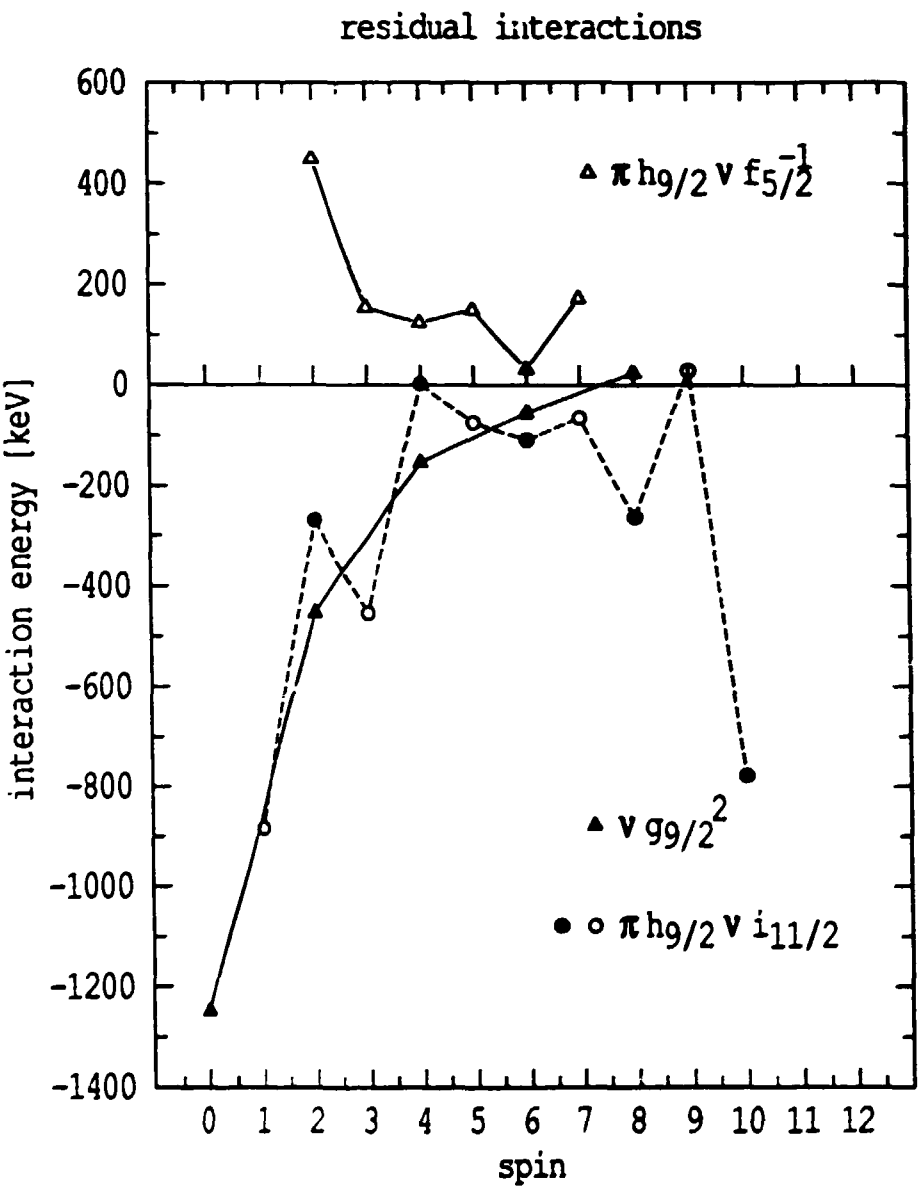

Figure 2. Typical residual reactions

modern terminology, the MONA mechanism[10]). This interaction, residual to the sum of the independent particle energies, is well understood[11] from the study of 2-particle multiplets. Examples are shown in figure 2. It can be generalised in terms of the overlap of the orbitals (better defined for higher j) as a function of the classical angle of orientation, cos θ_{12} between the aligning spins[11]. Its inclusion in the many-particle case involves traditional angular momentum recoupling (see ref[12] for examples).

Whilst the proton-neutron interaction is attractive, the aligned proton-neutron *hole* interaction is generally repulsive, hence utilisation of the $i_{13/2}^{-1}$ neutron configuration in conjunction with aligned protons is unlikely to be competitive. (A related argument is that the mass distribution of aligned particles is oblate whereas that of aligned holes is prolate.)

2.1.2 *The classical example – ^{212}Po.* The multiplet structure for j^2 and $\pi(j_1^2)\,\nu(j_1 j_2)$ is evident in the spectrum of $^{212}_{82+2}Po_{126+2}$ shown in figure 3. The reduced energy spacing between states obtained by the alignment of particles in a short range (pairing) interaction leads to the inverted parabolas, resulting in an isomer at spin 8^+. Similar isomers are known in many heavy nuclei near closed shells. In the $(j)^n$ cases particularly long-lived examples are observed near mid-shell because of seniority cancellation[13] and the consequent reduction in the B(E2) for $J_{max} \rightarrow J_{max-2}$ as discussed in the contributions of Piiparinen to this school[14]. In ^{212}Po alignment of the $(h_{9/2})^2_{8^+}$ protons in combination with the $(g_{9/2}\, i_{11/2})_{10^+}$ neutrons leads, because of the strong attractive p-n interaction, to the 65s α-decaying isomer[15]. Although discovered[16] in 1962, it does not as yet have a definitive spin assignment but the absence of γ-decays favours $J^\pi = 18^+$ [17].

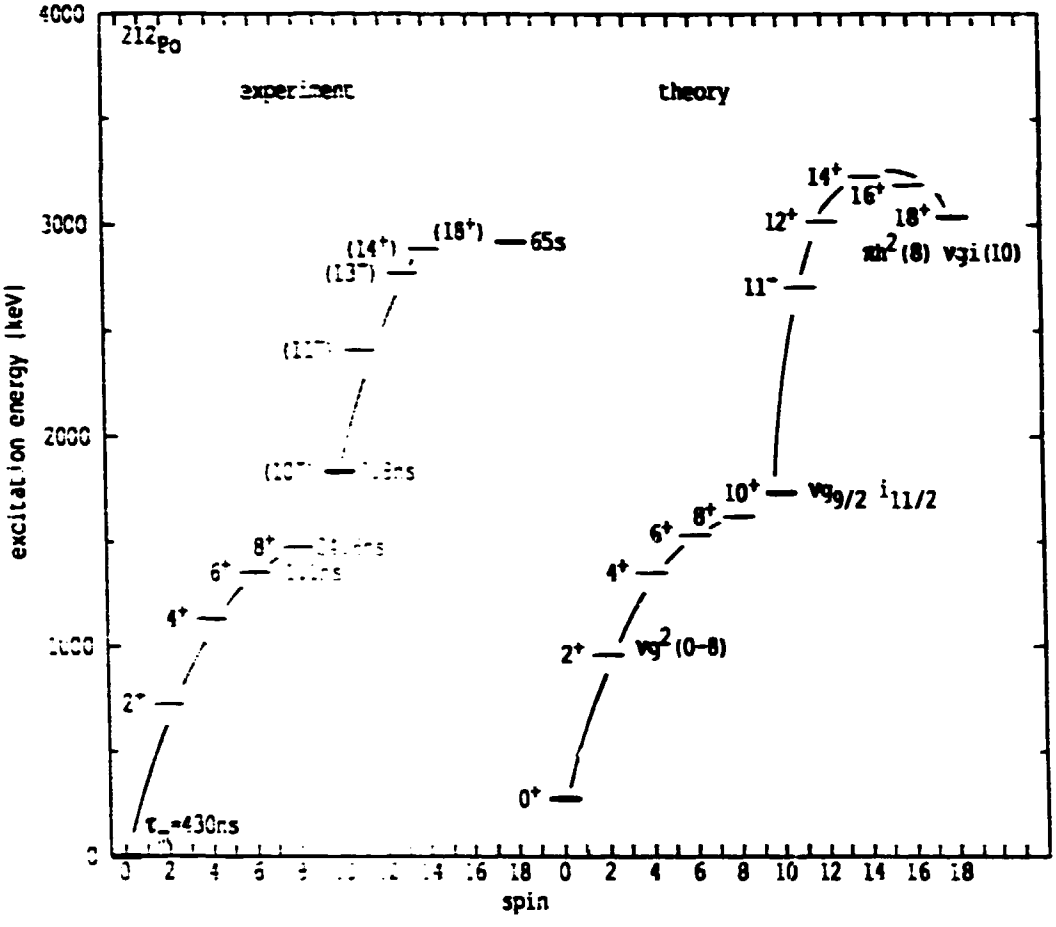

Figure 3. Experimental and theoretical yrast schemes for ^{212}Po

2.2 Core-excited Isomers - Examples

Figure 4 shows partial schemes of the main yrast states in the region of core excitations in $^{211}Rn_{125}$ and $^{212}Rn_{126}$, taken from previous work[18-20]. The striking feature, as well as the large number of isomers, is the presence of strongly enhanced E3 transitions connecting pairs of states, 30^+ and 27^- in ^{212}Rn, $63/2^-$ and $57/2^+$ in ^{211}Rn, for example. Obviously, whatever the structure of each of the upper states, the states to which they decay must have a *closely related* structure. Their g-factors are relatively low and approximately given by

$$g \approx (1.1\, J_\pi - 0.1\, J_\nu)/J \qquad (3)$$

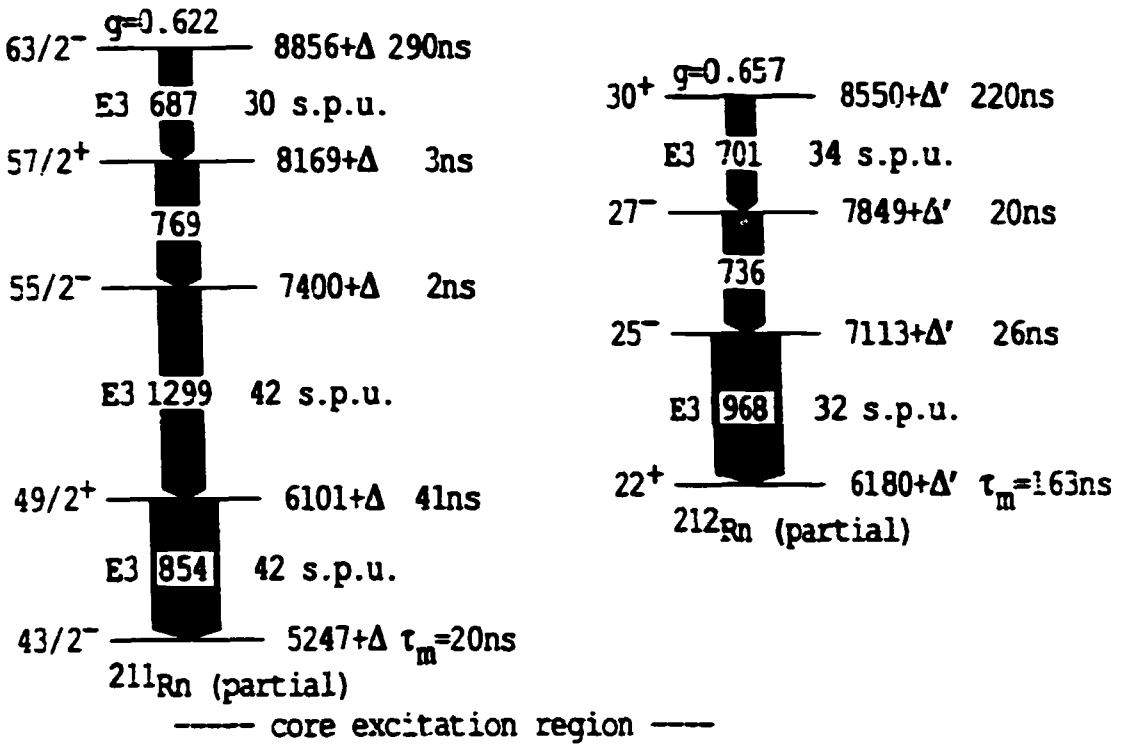

Figure 4. Partial schemes of ^{211}Rn and ^{212}Rn

consistent with core-excited configurations where about 40% of the angular momentum is provided by the neutrons (these are *double* core-excitations, giving four valence protons and two valence neutrons).

2.2.1 *DIPM assignments.* The 30^+ and 27^- states in ^{212}Rn have been associated[2-6] with oblate deformed states with configurations†

30^+; $\pi(h^2fi)_{18^-}\,\nu p^{-2}(gj)_{12^-}$; $\beta \sim -0.095$

27^-; $\pi(h^3i)_{17^-}\,\nu p^{-2}(gi)_{10^+}$; $\beta \sim -0.070$.

From simple angular coupling restrictions and the number of orbital changes, an E3 transition between such states is essentially forbidden! Similar considerations apply to the configurations and decay properties of

† suppressing, for simplicity, the individual spins. In the following we will use the abbreviations, for protons: h ≡ $1h_{9/2}$, i ≡ $1i_{13/2}$, f ≡ $2f_{7/2}$, for neutrons g ≡ $2g_{9/2}$, i ≡ $i_{11/2}$, j ≡ $1j_{15/2}$

the $63/2^-$ isomer in ^{211}Rn, which resembles the 30^+ isomer in ^{212}Rn with a partially aligned neutron hole $(f_{5/2})^{-1}_{3/2}$ added.

A second problem which confronts the DIPM is the small quadrupole moment measured[21] for the $63/2^-$ isomer in ^{211}Rn. Its magnitude is explained by the mixed shell model configurations, without requiring significant deformation[21,22]. A similar conclusion was reached[23] from the measurement of the quadrupole moment of the $65/2^-$ isomer in $^{213}_{87}Fr_{126}$ which also has a related configuration.

As shown by Matsuyanagi, Døssing and Neergård[3] the deformation energy in the DIPM accounts for a considerable portion of the shell-model residual interaction, although not in detail, and not for all cases. (A direct comparison between deformation energy and residual interactions for the configuration proposed for the 30^+ isomer in ^{212}Rn is given in ref[12].) As shown in figure 5, inclusion of the deformation dramatically improves the comparison between theory and experiment, compared to the pure "spherical" case. However, this improvement is misleading if it is taken to imply that deformation is a necessary component. Shell model calculations using semi-empirical shell model interactions give almost perfect agreement as also shown in figure 5, even up to the highest spin states. The point to be made here is that obviously there will be agreement between the leading-order configurations in both the deformed basis and the empirical shell model *for those states in which the deformed energy approximately reproduces the residual shell model interactions*. It is certainly unfair to expect more detailed agreement from the DIPM. The relevant question is whether deformation is the driving force and correspondingly, which description provides the more correct, or more compact approach?

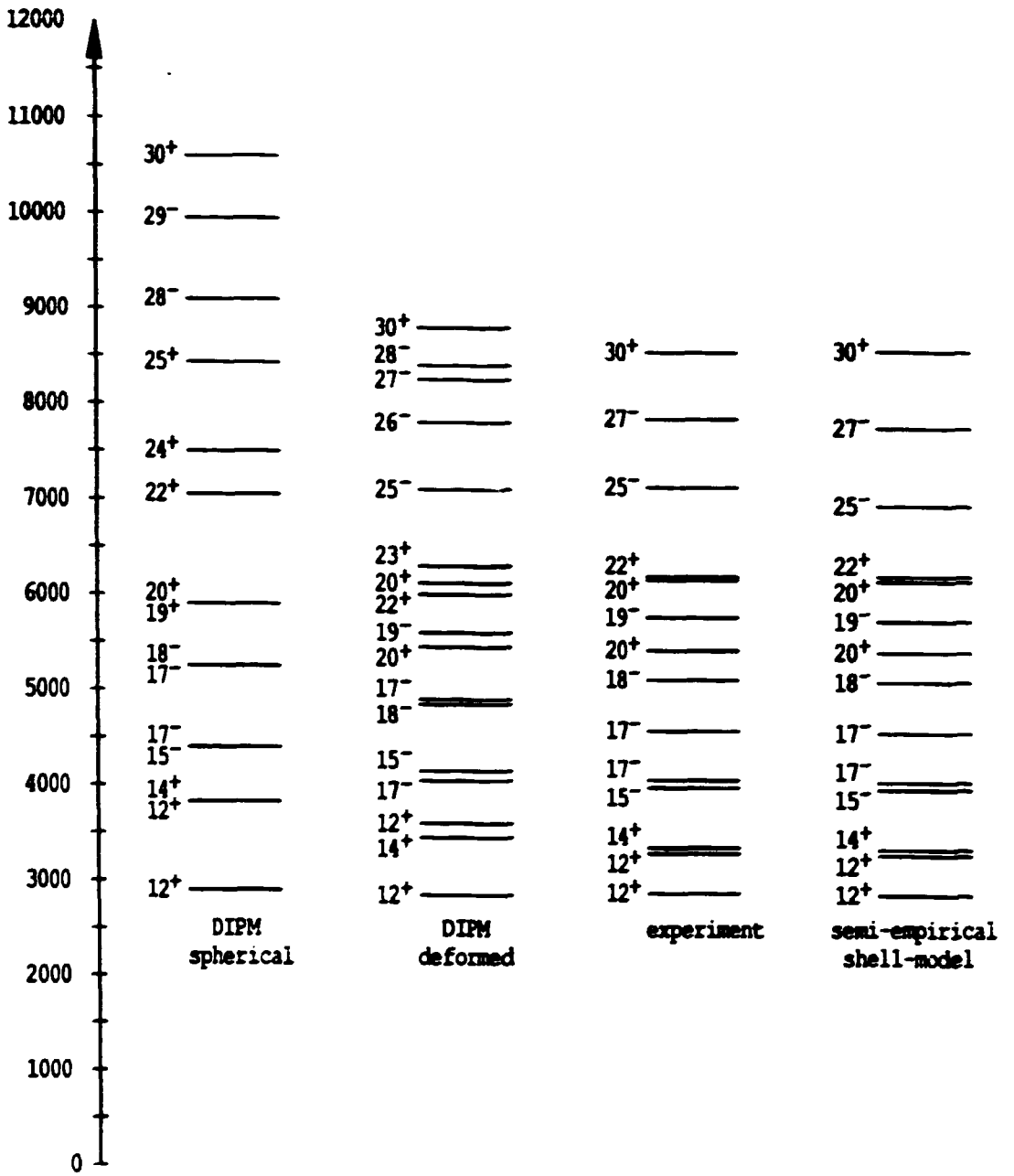

Figure 5. Spherical and Deformed yrast states (both from the DIPM) compared with experiment in ^{212}Rn. The levels on the right are the semi-empirical shell model calculations.

Collected in figure 6 are the known core-excited isomeric states for the N ≤ 126 isotopes of At, Rn and Fr, with their measured properties (E3 strengths and g-factors). The results are taken from published work[17-20, 24-30] except for the proposed 34⁺, 34 μs isomer in ^{212}Fr which was identified in recent measurements in our laboratory by Byrne et al[31]. At the conclusion of this talk I will also show our new results for ^{211}Rn and ^{212}Rn.

It should be apparent from figure 6 that there is a large number of core-excited isomers known and most are connected by very enhanced E3 transitions. In some cases enhanced E3 transitions occur in sequence, relating three or more states.

Also shown on the figure are excitation energies, g-factors and E3 strengths calculated within the semi-empirical shell-model (pioneered by Blomqvist and collaborators[32]) but modified to include coupling to the core octupole-vibration – an approach[27] we have labelled as MPOC (multi-particle, octupole-vibration coupling).

Table 1
Single-particle energies, energy depressions due to octupole coupling and wave functions

Nucleus	Empirical state	Energy [keV]	ΔE^{oct} a)	Wave function
^{209}Bi	$\pi \mid \tilde{i}_{13/2}\rangle$	1609	410	$0.912 \mid i_{13/2}\rangle + 0.365 \mid f_{7/2} \otimes 3^-\rangle$ $+ 0.19 \mid h_{9/2} \otimes 3^-\rangle$
	$\pi \mid \tilde{f}_{7/2}\rangle$	897	387	$0.952 \mid f_{7/2}\rangle + 0.3007 \mid (i_{13/2} \otimes 3^-)_{7/2}\rangle$
	$\pi \mid \tilde{h}_{9/2}\rangle$	0	15	$0.998 \mid h_{9/2}\rangle - 0.061 \mid (i_{13/2} \otimes 3^-)_{9/2}\rangle$
^{209}Pb	$\nu \mid \tilde{g}_{9/2}\rangle$	0	213	$0.977 \mid g_{9/2}\rangle + 0.214 \mid (j_{15/2} \otimes 3^-)_{9/2}\rangle$
	$\nu \mid \tilde{j}_{15/2}\rangle$	1422	426	$0.875 \mid j_{15/2}\rangle + 0.484 \mid (g_{9/2} \otimes 3^-)\rangle$

a) Energy depression due to particle-octupole vibration coupling.

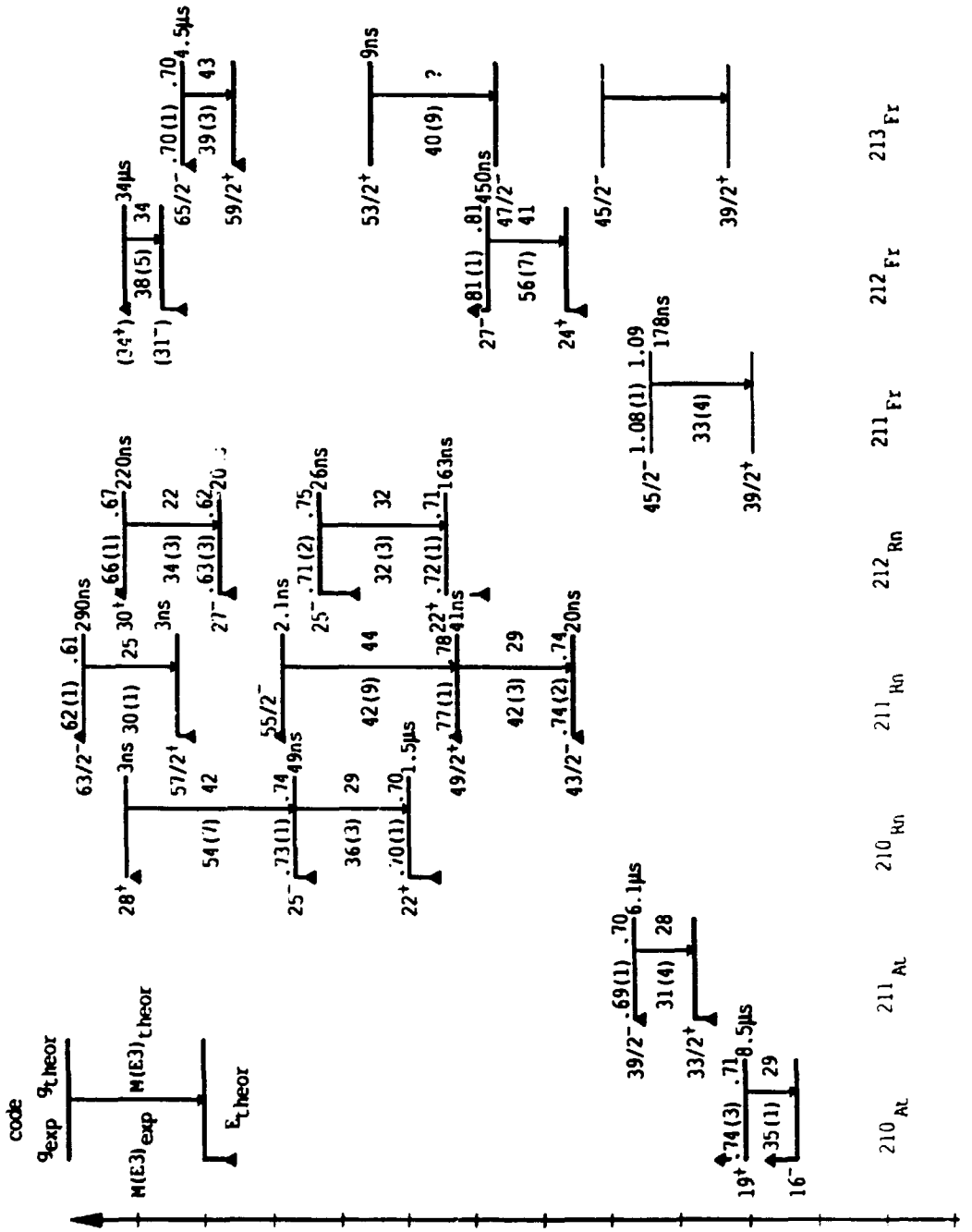

Figure 6 Core-excited states in At, Rn and Fr nuclei with $N \leq 126$. Also shown are the excitation energies, g-factors and E3 strengths (in s.p.*u.*) calculated in the MPOC model.

3.1 One-Particle Cases

Coupling to the 2.614 MeV, 3^- vibrational core of ^{208}Pb results in mixed configurations in the neighbouring odd-proton and odd-neutron nuclei ^{209}Bi and ^{209}Pb. Calculation of their properties provides a text-book example of particle-vibration coupling[33,34]. It involves, for example, solution of a 2×2 matrix for the calculation of the properties of the $J^\pi = 15/2^-$ state in ^{209}Pb. It is not a pure neutron $j_{15/2}$ configuration but rather, a state with $\nu j_{15/2}$ and $\nu g_{9/2} \otimes 3^-$ admixtures. (The coupled configuration will be indicated below with a tilde thus $\tilde{j}_{15/2}$.) As shown in table 1 significant admixtures are known for both odd-proton and odd-neutron configurations. The coupling strength, which, together with the unperturbed energies, determines the final admixtures, is not arbitrary but is deduced from the *amplitude of the oscillations* which can be related to the B(E3) of the $3^- \rightarrow 0^+$ core transition. The corresponding E3 transition in the coupled case is also enhanced since it can proceed via both core and single-particle transitions which also interfere. In general there will be a pair of mixed states

$$|J_i\rangle = \alpha\,|j_i\rangle + \beta\,|(j_f \otimes 3^-)_{J_i}\rangle$$

$$|J_f\rangle = \gamma\,|j_f\rangle + \delta\,|(j_i \otimes 3^-)_{J_f}\rangle$$

so that[24]

$$B(E3;\, J_i \rightarrow J_f) = \left[\alpha\gamma \frac{\hat{J}_f}{\hat{J}_i} \langle j_f \| T^3 \| j_i \rangle + \left\{ (-1)^{j_f + 3 - j_i} \beta\gamma + \frac{\hat{J}_f}{\hat{J}_i} \alpha\delta \right\} \sqrt{B(E3;3^- \rightarrow 0^+)} \right]^2$$

3.3 Multi-Particle Cases

The observation of enhanced E3 transitions between the core-excited states is an obvious indication that their configurations probably involve orbital changes of the style

$$\pi\,\tilde{i}_{13/2} \rightarrow \pi\,\tilde{f}_{7/2}$$

or $$\nu\,\tilde{j}_{15/2} \rightarrow \nu\,\tilde{g}_{9/2}$$

Extension from the 1-particle cases to the multi-particle case was carried out in an approximate form, in ref[27]. It involved first a summation of the single particle energies (obtained from empirical values corrected however for the octupole-vibration coupling (table 1), since it is included subsequently). Residual proton-neutron interactions are added but again, since the empirical values already contain octupole-coupled contributions,

Table 2
Eigenvectors of related core-excited states ^{211}Rn and ^{212}Rn (from ref[27])

	Amplitudes			
Basis states	$^{211}Rn, \frac{49}{2}^+$	$^{212}Rn, 25^-$	$^{211}Rn, \frac{63}{2}^-$	$^{212}Rn, 30^+$
	$+(\nu^{-2})_0$	$+(\nu^{-1})_{1/2}$	$+(\nu^{-1}i_{11/2})_7$	$+\nu i_{11/2}$
$\pi(h^2i^2)_{20}+\nu g$	0.560	0.527	–0.554	–0.606
$\pi(h^3i)_{17}\bar{}\nu j$	0.420	0.424	–0.512	0.441
$\pi(h^3i)_{17}\bar{}\nu g)_{43/2}\bar{}\otimes 3^-$	0.249	0.257	–0.268	–0.241
$(\pi(h^3f)_{14}{}^+ \nu j)_{43/2}- \otimes 3^-$	0.192	0.201	–0.193	–0.175
$\|\psi\rangle_-$	–0.039	–0.036	0.038	0.043
$\|\psi\rangle_+$	0.368	0.374	–0.319	–0.339
$\pi(h^3f)_{14}{}^+\nu g\otimes(3^-)^2$	0.128	0.137	–0.115	–0.110
$\pi(h^2(if)_{9}{}^-)_{17}\bar{}\nu j$	0.415	0.433	–0.368	–0.379
$\pi(h^2f^2)_{14}{}^+\nu j\otimes 3^-$	0.156	0.167	–0.120	–0.125
$\pi(h^2f^2)_{14}{}^+\nu g\otimes(3^-)^2$	0.130	0.137	–0.098	–0.106
$\|\chi\rangle_-$	–0.005	–0.009	0.001	–0.002
$\|\chi\rangle_+$	0.204	0.195	–0.205	–0.217
$\pi h^2((if)_{10}\bar{}\nu j_{15/2})_{33/2}$	0.052	0.062	–0.057	–0.058

$$|\psi\rangle_\pm = \left(\pi\left(h^2(if)_{9}{}^-\right)_{17}\bar{}\nu g\right)\otimes 3^- \pm \pi\left(h^2\left(i(f\otimes 3)_{13/2}\right)_{12}{}^+\right)\nu g \times 1/\sqrt{2(1\pm\delta_1)}, \quad \delta_1 = 0.84;$$

$$|\chi\rangle_\pm = \left(\pi\left(h^2(i^2\otimes 3^-)_9\bar{}\nu j \pm \pi(h^2i^2)_{20}{}^+\left(\nu j\otimes 3^-\right)_{9/2}\right)\right) \times / \sqrt{2(1\pm\delta_2)} \qquad \delta_2 = 0.69.$$

the theoretical values of Kuo and Herling[35] (which in general are less than the empirical values) are used. Finally off-diagonal elements are included – relatively small shell model values and the large octupole-vibration matrix elements. In comparison with the 1-particle case the main differences are specific angular momentum recoupling and a larger basis, giving usually a matrix of ~ 10 × 10. Diagonalisation of the matrix yields amplitudes as shown for typical states in table 2. From these amplitudes the g-factor and quadrupole moment can be calculated. The E3 transition rate is calculated from the explicit wave functions for a pair of states, which includes core transitions ($\doteq 3^- \rightarrow 0^+$), unperturbed single-particle transitions and interference. The good agreement obtained for a large number of cases as shown in figure 6 must provide strong support for the appropriateness of such a description.

It should be noted that the relationship between the 1- and many-particle case is non-linear as can be seen by comparing the *relative* amplitudes of say, the $g_{9/2} \otimes 3^-$ and $j_{15/2}$ components in table 2 with those in table 1.

It is also useful to view the wave function of the $49/2^+$ state of table 2 in an approximate notation, since it illustrates an important effect governing the formation of many of the core-excited isomers.

It could be written approximately as the combination of two components

$$\left\{[\text{CORE}]\,\pi\,\tilde{i}_{13/2}\right\}_{20^+}\nu\tilde{g}_{9/2} \quad \text{and} \quad \left\{[\text{CORE}]\,\pi\,\tilde{f}_{7/2}\right\}_{17^-}\nu\tilde{j}_{15/2}.$$

If these configurations had been orthogonal they would have been, because of the differences in single-particle energies, nearly degenerate. However they mix automatically through the octupole coupling. Comparable mixing was invoked by a Stockholm group[36,37] to explain the properties of isomers in At nuclei. In essence they solved for the amplitudes required to explain simultaneously the g-factor and E3 rate. However, as we have shown, the mixing arises naturally through the octupole coupling.

3.4 Relationships

Shown in fig 7 are the proposed relationships between the main core excited states in the Rn nuclei and their connection to the At isotopes and the Fr isotopes. Within ^{211}Rn for example, the higher spin states are obtained by the additional core-excitation $(f_{5/2}^{-1}\, i_{11/2})_{j_{max}\text{-}1}$ where only partial alignment is favoured because of the otherwise repulsive interactions described in section 2.1.

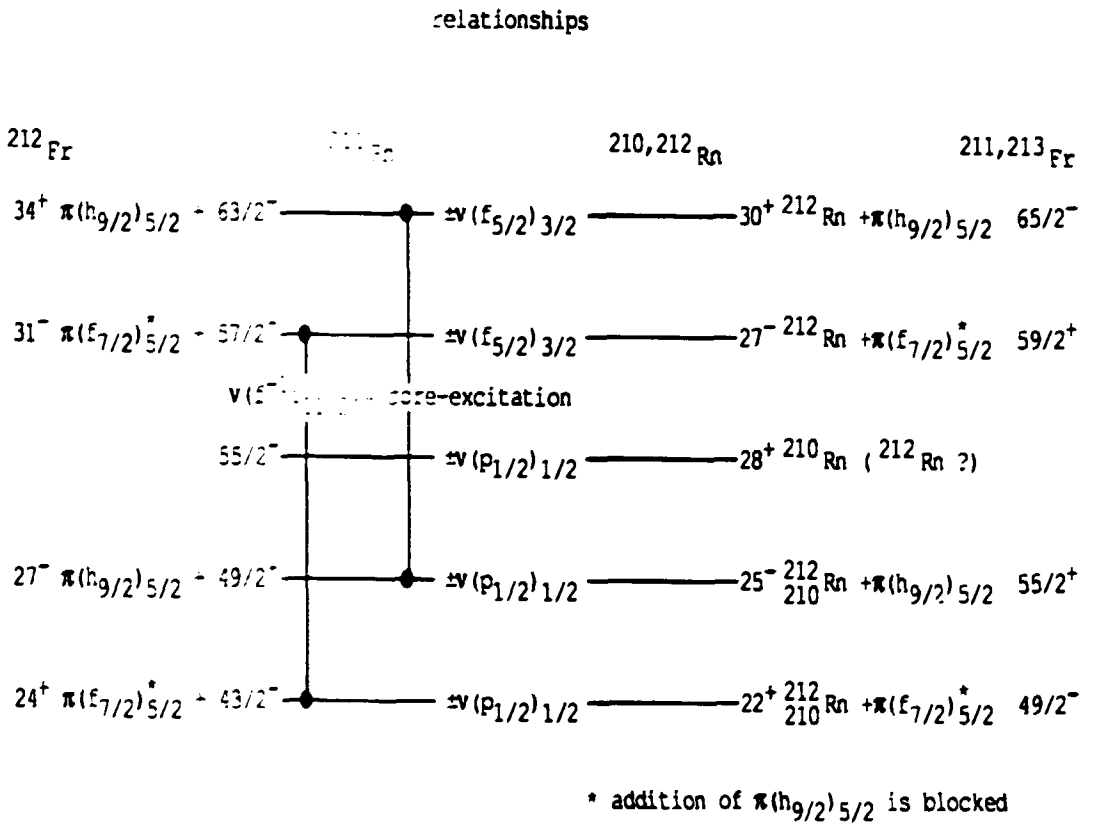

Figure 7. Relationships between core-excited isomers.

3.5 Limitations

Several critical comments could be made regarding the simple model presented. Firstly, it should be noted that the g-factors are not specifically sensitive to the octupole mixed components since the g-factor of the 3- octupole vibration is 0.54 comparable to the "final" value obtained for

double core excitations when 60% of the angular momentum is provided by the protons, and 40% by the neutrons (see equation 3). Secondly, no account has been taken of the effect of blocking on the core octupole-vibration. (Although blocking is included in estimating the unperturbed component energies.) Since the 3^- vibration in ^{208}Pb is a coherent admixture of particle-hole components, occupation of specific proton and neutron orbitals to form the multi-particle case will reduce the collectivity. However, no one amplitude dominates in either the vibrational, or multi-particle components, hence the blocking is not severe. Nevertheless, it is one aspect which is properly included in a more formal theory. A compensatory effect which might be covering a discrepancy due to blocking is that the collectivity of the "core" is likely to increase as particles are added to ^{208}Pb (see for example the analysis of ref[38]) so that any reduction due to blocking may have been masked by an increased core collectivity. On average, the MPOC model underestimates the B(E3) values by ~18%.

4. EXTENSION TO HIGHER SPIN IN ^{211}Rn and ^{212}Rn

From the MPOC model we can anticipate yrast states in ^{212}Rn and ^{211}Rn decaying by enhanced E3 transitions to the 30^+ and $63/2^-$ core excited isomers, respectively. Their configuration in the shorthand notation would be as below.

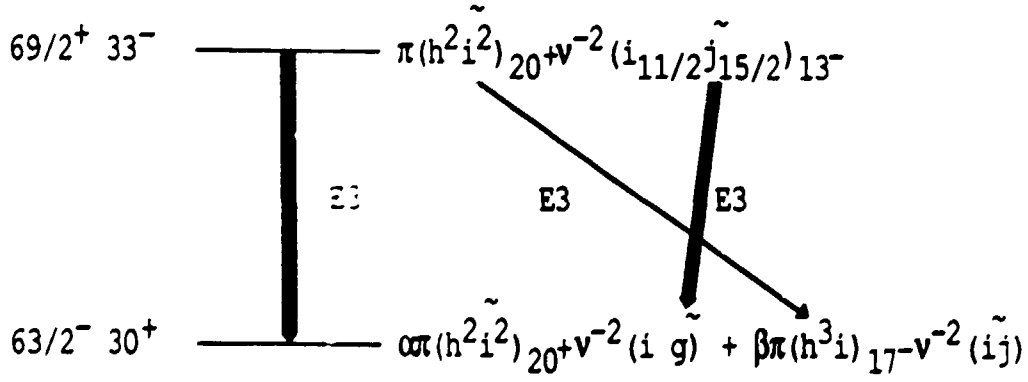

If no more core excitations are allowed, or at least unfavoured in energy, the maximum spins one can form from the valence orbitals in ^{212}Rn are $J^{\pi} = 34^{+}$; $\pi(h^2i^2)_{20^+}\, \nu^{-2}\, (\tilde{j}^{\,2}_{15/2})_{14^+}$ which is calculated to be near 11 MeV and, at higher energy $J^{\pi} = 35^{-}$; $\pi\,(hi^3)_{21^-}\ \nu^{-2}\, (\tilde{j}^{-2}_{15/2})_{14^+}$. In ^{211}Rn the $J^{\pi} = 71/2^{-}$ partner to the 34^{+} state is expected to be yrast but the level scheme is likely to be more fragmented, since, depending on partial or complete alignment of the $f_{5/2}$ neutron hole, several states with spin between $71/2^{+}$ and $75/2^{+}$ can be formed.

4.1 New Measurements

Using two new facilities at the Australian National University 14 UD Pelletron accelerator, a 7 (or 6)-element Compton suppressor array, named CAESAR, and a superconducting, solenoidal electron spectrometer, SUPER-E, we have carried out new measurements[40] probing the valence spin limit in ^{211}Rn and ^{212}Rn.

In the γ-ray measurements, retention of time information for detected γ-rays allows the construction of all γ-γ-time relationships and therefore the unambiguous placement of transitions above and below isomeric states. The electron spectrometer[39] was operated in LENS mode with momentum matching (through software restrictions on the matrix of magnetic field vs Si(Li) detector energy, constructed from the event-by-event data). A significant improvement in spectrum quality was therefore obtained by eliminating backscattered and other continuum events.

Transitions observed feeding the 30^{+} isomer in ^{212}Rn and the $63/2^{-}$ isomer in ^{211}Rn, obtained from γ-γ-time data collected during bombardment of ^{198}Pt by a pulsed ^{18}O beam, are shown in the upper panel of figure 8. In each case the main yrast intensity is carried by a single transition – 1061 keV in ^{211}Rn and 1117 keV in ^{212}Rn. (Both transitions had been observed weakly in previous work[5,19].) The lower panels show prompt and delayed gates on the 1061 keV transition which place the 1166 keV transition above it, and show clearly the decay of the $63/2^{-}$ isomer.

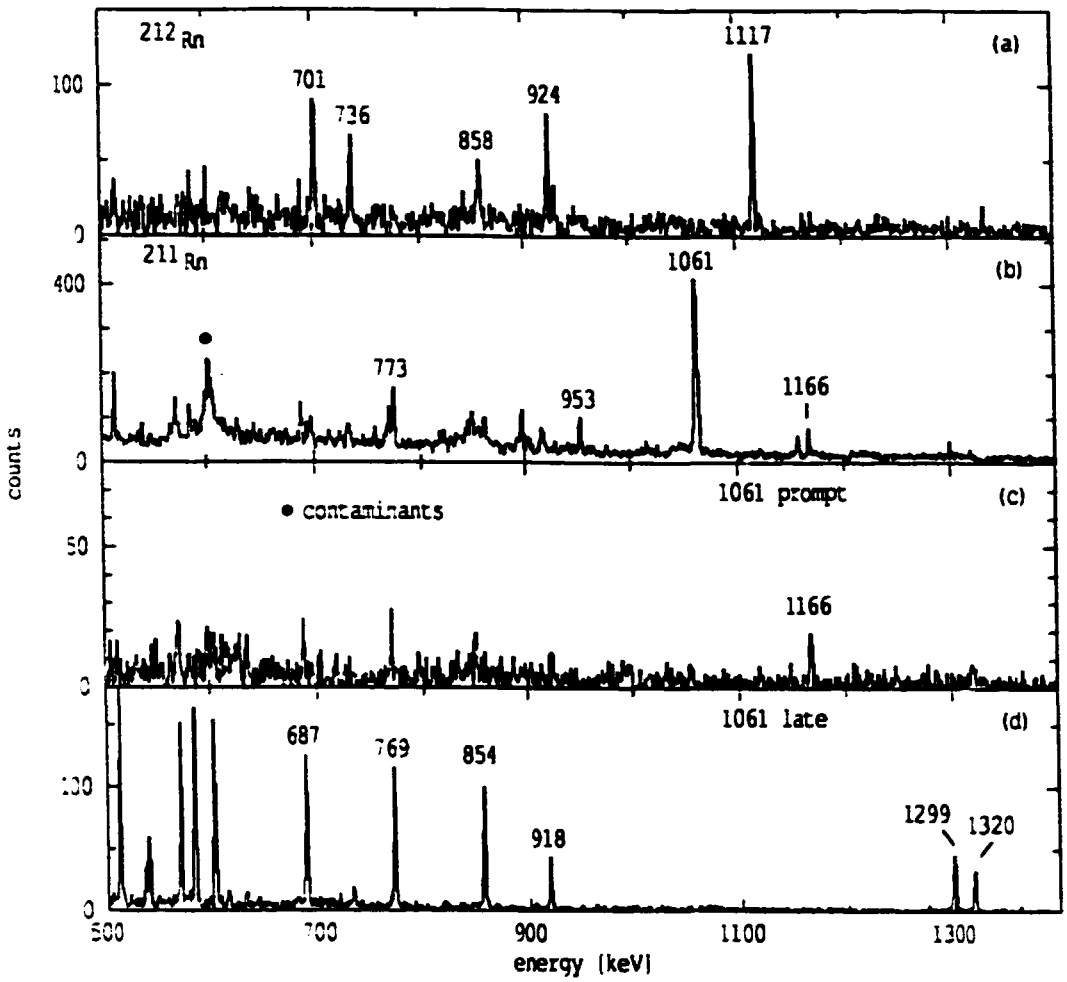

Figure 8(a) Transitions preceding the 30^+ isomer in ^{212}Rn gated on the 701, 736 and 968 keV cascade transitions. (The 701 and 736 appear weakly in this spectrum because of the short lifetime of the 25^- state which decays by the 968 transition.)

(b) Transitions preceding the $63/2^-$ isomer in ^{211}Rn gated on the 687, 769 and 1299 keV cascade transitions.

(c) Prompt gate (±24ns) on the 1061 keV transition.

(d) Spectrum of γ-rays delayed with respect to the 1061 keV transition.

Time spectra for individual transitions are given in figure 9 showing the absence of long-lived components in the 1061 and 1117 keV transitions, in contrast to the transitions depopulating the $63/2^-$ and 30^+ isomers. Each does show, however, a clear short lifetime. Fits to these curves, from which lifetimes of 13 ns and 7 ns for the new isomers in ^{211}Rn and ^{212}Rn were extracted are shown in figure 10. The results are given in table 3.

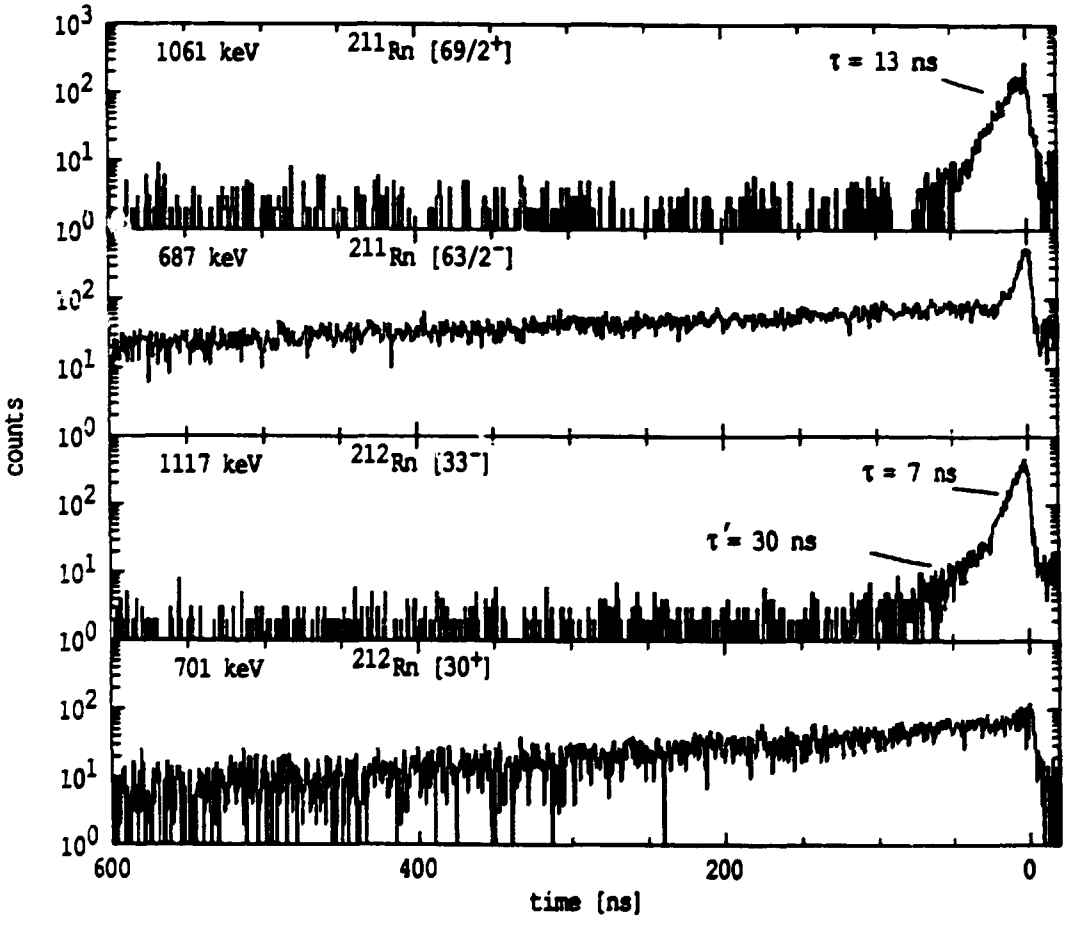

Figure 9 Time spectra with gates on individual transitions in ^{211}Rn and ^{212}Rn as indicated. (The small prompt component in the 687 gate occurs through a contaminant.)

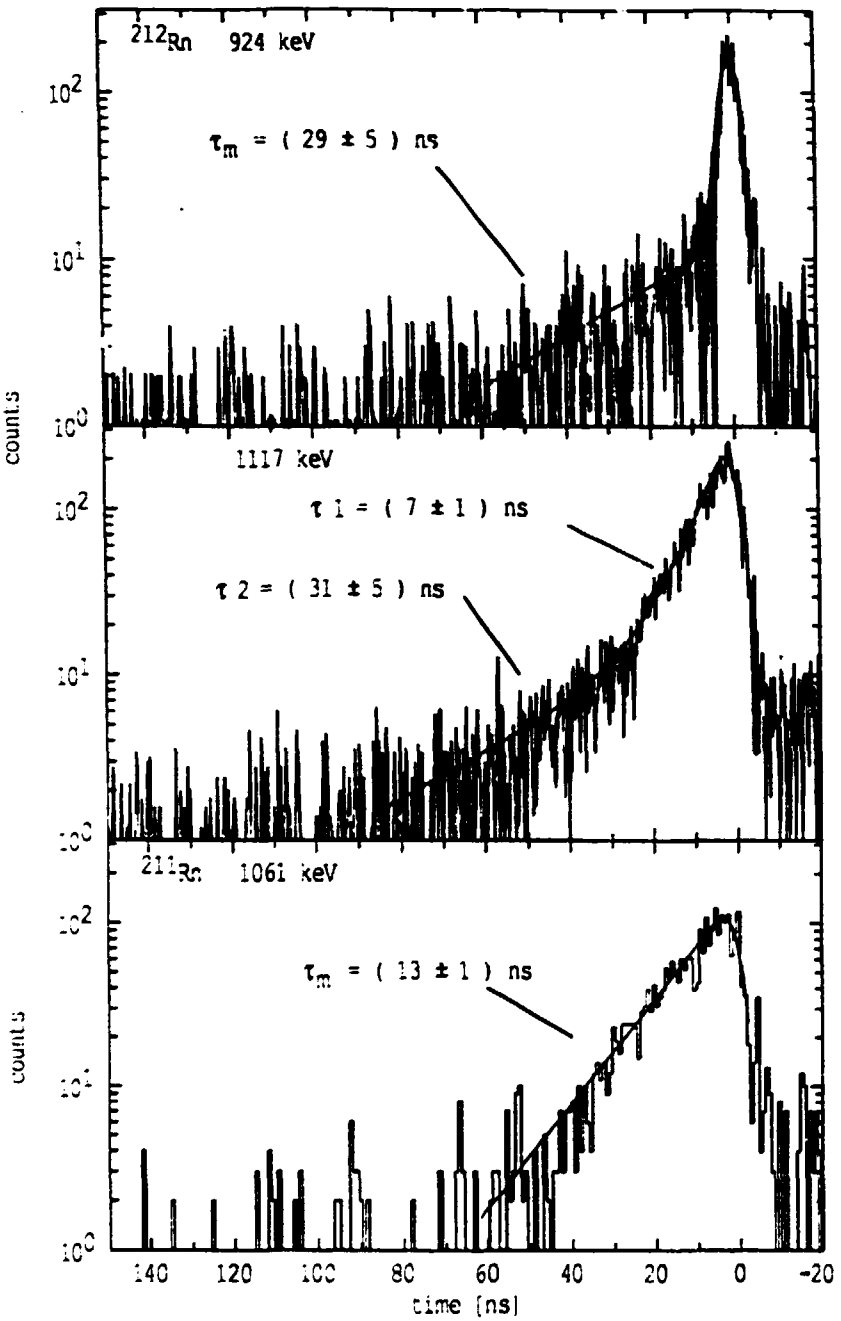

Figure 10 Fits to the short lifetimes in ^{211}Rn and ^{212}Rn.

Examples of associated γ-ray and conversion electron spectra are shown in figure 11. By gating in the short delayed time region, away from the prompt peak, the peak-to-background ration in the γ-ray and electron spectra can be optimised. The electron lines from the 1061 and 1117 keV transitions are clear. The K and L conversion coefficients summarised in table 3 establish E3 multipolarity.

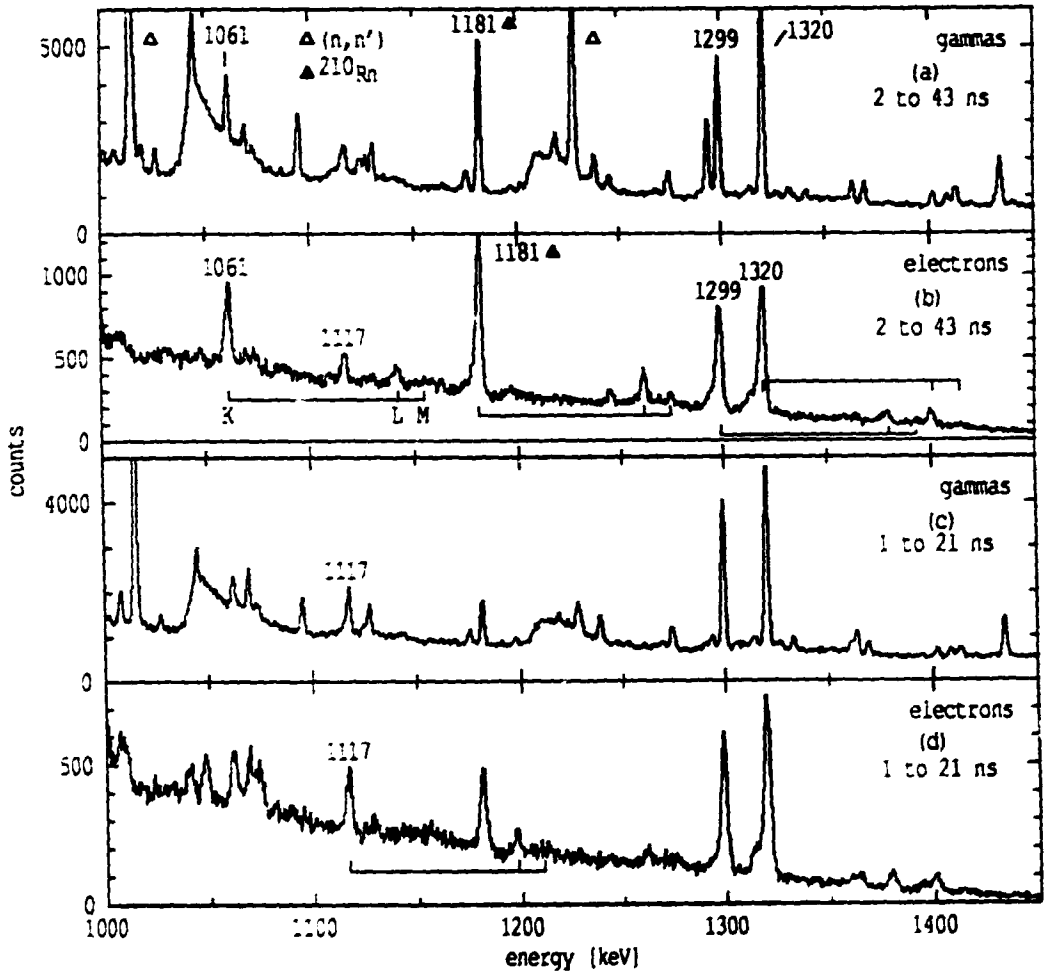

Figure 11 (a) and (b) Corresponding gamma-ray and electron spectra with time gates as shown. Beam energy of 96 MeV optimised for ^{211}Rn population. The 1181, 1299 and 1320 keV lines are of E3 multipolarity.

(c) and (d) Corresponding gamma-ray and electron spectra with time gates as shown. Beam energy of 92 MeV to increase population of ^{212}Rn.

Table 3
Properties of high-spin isomers in radon isotopes

Nuclide	E_γ (keV)	initial state	γ-ray anisotropy[a]	conversion coefficients x 100					τ (ns)
				type	exp	M1	E2	E3	
^{211}Rn	1061	9916+Δ	1.4(1)	K	1.31(7)	1.84	0.578	1.24	13(1)
				K/L	3.5(4)	5.84	4.85	3.48	
^{212}Rn	1117	9969+Δ'	1.2(1)	K	1.02(5)	1.61	0.527	1.12	7(1)
				K/L	3.9(5)	5.85	4.96	3.64	

a) ratio of 145°/97° detectors

From table 4 the E3 decays for the new isomers, assigned as $J^\pi = 69/2^+$ and 3
in ^{211}Rn and ^{212}Rn are seen to be strongly enhanced. Excitation energies a
transition strengths agree well with the predictions of the MPOC model. A
shown in the same table similar agreement is obtained for the $63/2^-$ and 3
states (results taken from ref[27]) hence a good description is obtained for
sequence of three connected states in both nuclei.

Table 4
Comparison of experimental and theoretical properties

Nuclide	J^π	Excitation[a] (keV)		M(E3) s.p.u.	
		exp	theory[b]	exp	theory[b]
211Rn	$69/2^+$	9916+Δ	10031	33(3)	38
	$63/2^-$	8856+Δ	8882	30(1)	25
	$57/2^+$	8169+Δ	8064		
^{212}Rn	33^-	9669+Δ'	9702	43(6)	41
	30^+	8550+Δ'	8571	34(3)	22
	27^-	7489+Δ'	7761		

a) results for $63/2^-$ and 30^+ states from ref [27]
b) MPOC model

Candidates have also been observed for states with the valence-spin limit. These will be discussed elsewhere.

5. SUMMARY AND COMMENTS

Overall, it seems that a detailed description has been obtained of the core-excited isomers in the Rn, At and Fr isotopes. The factors which govern the optimum configuration for yrast states are the attractive proton-neutron interaction and the particle-octupole-vibration coupling. At present it does not seem necessary to invoke oblate deformation in the formation of yrast isomers.

From the theoretical point of view inclusion of an explicit octupole degree of freedom in the deformed independent particle model is mandatory since without its presence, of necessity, only the oblate-quadrupole deformed space is being explored.

Future experimental work involves extension to higher spins, possibly using continuum γ-ray techniques with the prospect of investigating the region above the limit of valence spin where collective structures quadrupole, or octupole, or coupled, could occur.

References

1) Ploszajcak, M., Toki, H. and Faessler A., J. Phys. G: Nucl. Phys. 4, 743 (1978).

2) Andersson, C.G., Hellström, G., Leander, G., Ragnarsson, I., Åberg, S., Krumlinde, J., Nilsson, S.G. and Szymański, Z., Nucl. Phys., A309, 141 (1978).

3) Matsuyanagi, K., Døssing, T. and Neergård, K., Nucl. Phys. A307, 253 (1978).

4) Dudek, J., Szymanski, Z. and Werner, T., Phys. Rev. C 23, 920 (1981).

5) Lönnroth, T., Beausang, C.W., Fossan, D.B., Hildingsson, L., Piel Jr., W.F. and Warburton, E.K., Physica Scripta 39, 56 (1989).

6) de Voigt, M.J.A., Dudek, J. and Szymanski, Z., Rev. Mod. Phys. 55, 949 (1983).

7) Hamamoto, I. and Mottelson, B., Proceedings of the "Symposium on the Occasion of the 40th Anniversary of the Nuclear Shell Model", May 25-27, 1989, Argonne National Laboratory.

8) Häusser, O., Mahnke, H.E., Alexander, T.K., Andrews, H.R., Sharpey-Schafer, J.F., Swanson, M.L., Ward, D., Taras, P. and Keinonen, J., Nucl. Phys. A379, 287 (1982).

9) Neergard, K., Døssing, T. and Sagawa, H., Physics Letters B99, 191 (1981).

10) Faessler, A., Ploszajczak, M. and Sandhya Devi, K.R., Phys. Rev. Lett. 36, 1028 (1976).

11) Schiffer, J.P. and True, W.W., Rev. Mod. Phys. 48, 191(1976).

12) Byrne, A.P. and Dracoulis, G.D., Nucl. Phys. A391 1 (1982).

13) de Shalit, A. and Talmi I., Nuclear Shell Theory, (Academic Press, NY 1963) eqn (28.40) p.315.

14) M. Piiparinen et al., these proceedings.

15) Glendenning, N.K., Phys. Rev. 127, 923 (1962).

16) Perlman, I., Asaro, F., Ghiorso, A., Larsh, A. and Latimer R., Phys. Rev. 127 197 (1962).

17) Poletti, A.R., Dracoulis, G.D., Byrne, A.P. and Stuchbery, A.E., Nucl. Phys. A473, 595 (1987).

18) Horn, D. et al., Phys. Rev. Lett. 39, 389 (1977).

19) Dracoulis, G.D., Fahlander, C. and Poletti, A.R., Phys. Rev. C24, 2386, (1981).

20) Poletti, A.R., Dracoulis, G.D., Byrne, A.P., Stuchbery, A.E., Poletti, S.J. and Gerl, J., Phys. Lett. 154B, 263 (1985); Nucl. A442, 153 (1985).

21) Dafni, E., Hass, M., Naim, E., Rafailovich, M.H., Berger, A., Grawe, H. and Mahnke, H.-E., Phys. Rev. Lett. 55, 1269 (1985).

22) Sagawa, H. and Arima, A., Phys. Lett. 202B, 15 (1988).

23) Hardeman, F., Neyens, G., Scheveneels, G., Nouwen, R., S'Heeren, G., Van Den Bergh, M., Coussement, R., Byrne, A.P., Müsselar, R., Hübel, H. and Baldsiefen, G., to be published.

24) Byrne, A.P., Dracoulis, G.D., Fahlander, C., Hübel, H., Poletti, A.R., Stuchbery, A.E., Gerl, J., Davie, R.F. and Poletti, S.J., Nucl. Phys. A448, 137 (1986).

25) Byrne, A.P., Musseler, R., Hübel, H., Murzel, M., Theine, K., Schmitz, W., Maier, K.H., Kluge, H., Grawe, H. and Haas, H., Phys. Lett. B217, 38 (1989).

26) Poletti, A.R., Dracoulis, G.D., Fahlander, C. and Morrison, I., Nucl. Phys. A380, 335 (1982).

27) Poletti, S.J., Dracoulis, G.D., Poletti, A.R., Byrne, A.P., Stuchbery, A.E. and Gerl, J., Nucl. Phys. A448, 189 (1986).

28) Maier, K.H., Leigh, J.R., Pühlhofer, F. and Diamond, R.M., Phys. Lett. B 35, 401 (1971).

29) Rahkonen V., Bergström, Blomqvist, J., Knuuttila, O., Rensfelt, K.-G., Sztarkier, J. and Westerberg, K., Z. Phys. A284, 357 (1978).

30) Dracoulis, G.D., Steed, C.A., Byrne, A.P., Poletti, S.J., Stuchbery, A.E. and Bark, R.A.,Nucl. Phys. A462, 576 (1987).

31) Byrne, A.P., Dracoulis, G.D., Schiffer, K.J., Davidson, P.M., Kibédi, T., Fabricius, B., Baxter, A.M. and Stuchbery, A.E., ANU-P/1061, submitted to Physical Review C.

32) See for example, ref [29].

33) Bohr, A. and Mottelson, B.R., "Nuclear Structure" (Benjamin, 1975) Vol II, Chaper 6.

34) Hamamoto, I., Physics Reports 10, 63 (1974).

35) Kuo, T.T.S. and Herling, G.H., Naval Research Laboratory, Washington, report 2258 (1971).

36) Bergström, I., Blomqvist, J., Carlé, P., Fant, B., Källberg, A., Norlin, L.O., Rensfelt, K.-G. and Rosengård, U., Phys. Scripta 31, 333 (1985).

37) Bergström, I. and Fant, B., Phys. Scripta 31, 26 (1985).

38) Dracoulis, G.D., Riess, F., Stuchbery, A.E., Bark, R.A., Gupta, S.L., Baxter, A.M. and Kruse, M., Nucl. Phys. A493, 145 (1989).

39) Kibédi, T., Dracoulis, G.D. and Byrne, A.P., Nuclear Instruments and Methods in Physics Research (in press).

40) Dracoulis, G.D., Davidson, P.M., Byrne, A.P., Fabricius, B., Kibédi, T., Stuchbery, A.E., Poletti, A.R. and Schiffer, K.J., Phys. Lett. (in press).